Implications of graded reductions in CLN6's anti-aggregate activity for the development of the neuronal ceroid lipofuscinoses

Arisa Yamashita[#], Yuki Shiro[#], Yuri Hiraki, Takatoshi Yujiri, Tetsuo Yamazaki*

Department of Molecular Cell Biology and Medicine, Graduate School of Biomedical Sciences, Tokushima University, 1-78-1, Sho-machi, Tokushima 770-8505, Japan

# equally contributed

* Corresponding author. TEL: +81 88 633 7886 FAX: +81 88 633 9550

E-mail address: tyamazak@tokushima-u.ac.jp (T. Yamazaki)

Abstract

CLN6, spanning the endoplasmic reticulum transmembrane, is a protein of unknown function. Mutations in the CLN6 gene are linked to an autosomal recessively inherited disorder termed CLN6 disease, classified as a form of the neuronal ceroid lipofuscinoses (NCL). The pathogenesis of CLN6 disease remains poorly understood due to a lack of information about physiological roles CLN6 plays. We previously demonstrated that CLN6 has the ability to prevent protein aggregate formation, and thus hypothesized that the abrogation of CLN6's anti-aggregate activity underlies the development of CLN6 disease. To test this hypothesis, we narrowed down the region vital for CLN6's anti-aggregate activity, and subsequently investigated if pathogenic mutations within the region attenuate CLN6's anti-aggregate activity toward four aggregation-prone αB-crystallin (αBC) mutants. None of the four αBC mutants was prevented from aggregating by the Arg106ProfsX truncated CLN6 mutant, the human counterpart of the *nclf* mutant identified in a naturally occurring mouse model of late infantile-onset CLN6 disease. In contrast, the Arg149Cys and the Arg149His CLN6 mutants, both associated with adult-onset CLN6 disease, blocked aggregation of two out of and all of the four αBC mutants, respectively, indicating that CLN6's anti-aggregate activity is differentially modulated according to the substitution pattern at the same amino acid position. Collectively, we here propose that the graded reduction in CLN6's anti-aggregate activity governs the clinical course of late infantile- and adult-onset NCL.

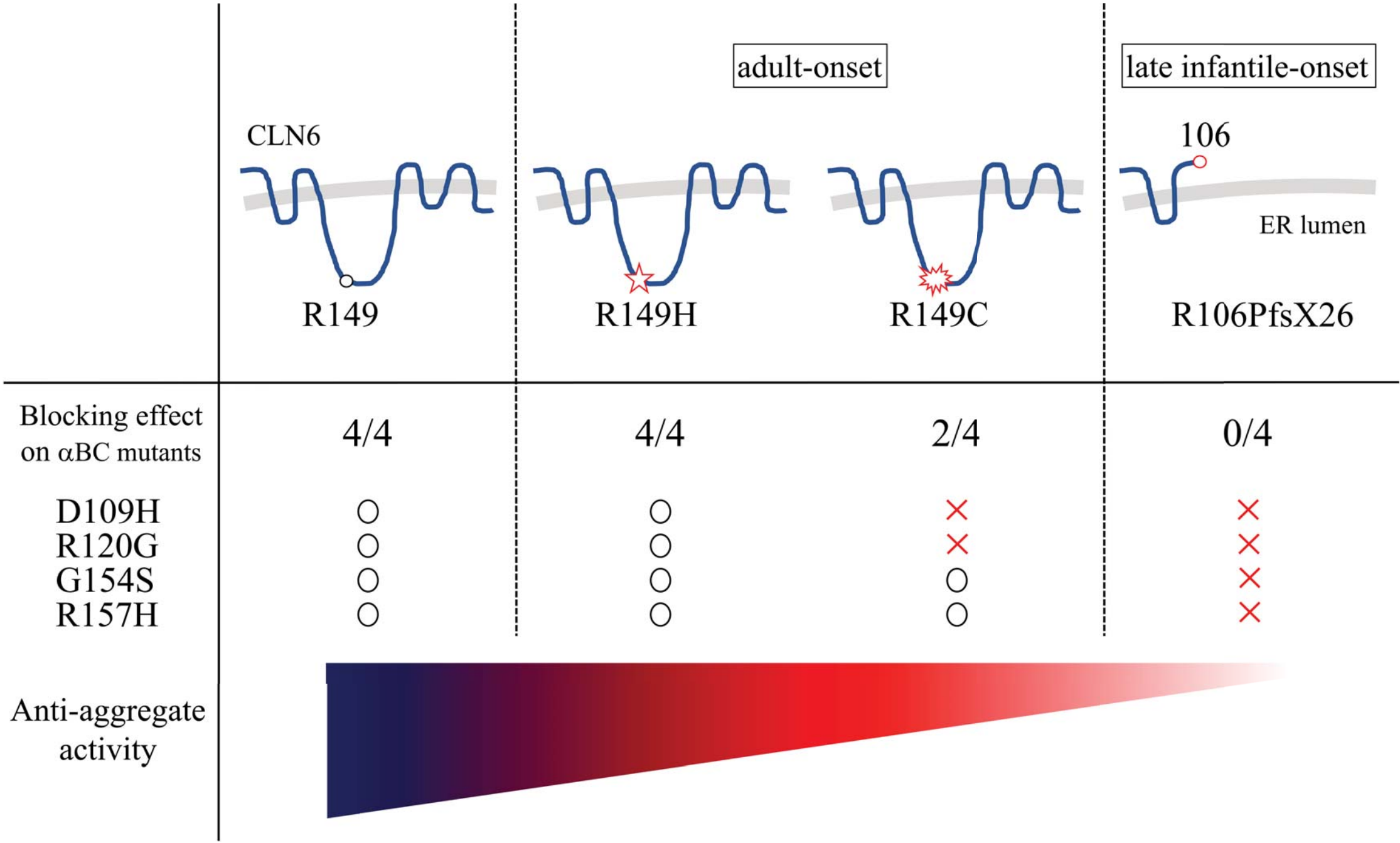
adult-onset
late infantile-onset
CLN6
106
ER lumen
R149
R149H
R149C
R106PfsX26
Blocking effect on αBC mutants
4/4
4/4
2/4
0/4
D109H
R120G
G154S
R157H
Anti-aggregate activity

1. Introduction

CLN6 is an endoplasmic reticulum transmembrane protein, and mutations in the CLN6 gene are responsible for the development of CLN6 disease, a form of NCL [1–8]. NCL are a group of hereditary neurodegenerative disorders, characterized by shared clinical manifestations such as psychomotor deterioration, epileptic seizures, progressive visual impairment, ataxia, and reduced lifespan. Histologically, intralysosomal accumulation of autofluorescent ceroid lipopigments is commonly found in patients with NCL. NCL are heterogeneous in the disease onset and clinical course. CLN6 disease is indeed subdivided into late infantile- and adult-onset subtypes [9,10]. Coupled with a lack of information about physiological roles of CLN6, the pathogenesis of CLN6 disease has been largely unknown. We previously revealed that CLN6 blocks aggregate formation mediated by a pathogenic αBC mutant [11]. This finding led us to hypothesize that dysfunction of CLN6 causes a buildup of protein aggregates, leading to the development of CLN6 disease. In fact, protein aggregates positive for p62, an autophagy receptor, were detected in the brain of the *nclf* mouse, a naturally occurring model of late infantile-onset CLN6 disease, arguing for our hypothesis [12]. In order to test the hypothesis, we here determined if anti-aggregate activity of pathogenic CLN6 mutants is decreased compared with that of wild-type CLN6. Because no physiological substrates of CLN6 have been identified at present, we employed four disease-causing αBC mutants, identified in patients of αB-crystallinopathy presenting with different clinical symptoms, as model target proteins of CLN6. Based on our data, we here propose that graded reductions in CLN6's anti-aggregate activity governs the clinical outcomes of CLN6 disease.

2. Materials and methods

2.1. Expression vectors

The expression vector construction of pEGFP-N1-R120G αBC mutant (R120G-EGFP), pcDNA4/myc-αBC (WTαBC) and pcDNA4/myc-CLN6 (CLN6) was described previously [11,13]. The DNA fragment encoding the D109H, G154S, R157H αBC mutants were generated by recombinant PCR. In each mutant, two fragments (Fragment 1 and Fragment 2) were generated by two sets of primers (Table S1) and WTαBC. And then, these fragments were used as templates for the second amplification with primers, 5'-CGGAATTCACCATGGACATCGCCATCC-3' and 5'-CGGTCGACCATTTCTTGGGGGCTGCG-3'. The final PCR products were gel-isolated, digested with BglII/PstI, and then cloned in frame into the BglII/PstI-digested pEGFP-N1 vector (TAKARA Bio). To construct pcDNA4/myc-R106PfsX26 CLN6 mutant (106fsX), performed sequential PCR used by PrimeSTAR Mutagenesis Basal Kit (TAKARA Bio). The first PCR used CLN6 and primers, "316insC-Fwd" and "316insC-Rev" (Table S2), and the second PCR used the first PCR product and primers, "106fsX-Fwd" and "106fsX-Rev" (Table S2). Then, the final product digested with HindIII/EcoRI and cloned in frame into the HindIII/EcoRI-digested pcDNA4/myc vector (Invitrogen). Other CLN6 mutants were generated by PrimeSTAR Mutagenesis Basal Kit (TAKARA Bio), using two primers (Table S3) and CLN6 as a template. All the constructs were subjected to DNA sequencing.

2.2. Cell culture and transfection

HeLa cells were grown in DMEM (WAKO, Tokyo, Japan) supplemented with 10% fetal bovine serum at 37 °C in a humidified cell culture incubator with 5% CO_2. For transfection, the cells were seeded at 1.5×10^4 cells per well onto 24-well plates 20 h prior to transfection. The cells in each well were transfected with single (0.4 μg) or

two different (0.2 μg each) expression vectors mixed with 1.2 μl of polyethyleneimine (PEI) “Max” (Polysciences).

2.3. Immunoblotting assays

At 16 h post-transfection, HeLa cells were lysed with RIPA buffer (100 mM Tris (pH 7.5), 150 mM NaCl, 2 mM EDTA, 1% TrironX-100, 1% DOC, 0.1% SDS and protease inhibitor cocktail), incubated on ice for 30 min, then centrifuged at 14,800 rpm for 10 min. Soluble fraction was collected, mixed with 2×Laemmli sample buffer (0.5 mM Tris-HCl (pH 6.8), 2.5% SDS, 25% glycerol, 2.5% 2-mercaptoethanol and 5% bromophenol blue), heated at 95 °C for 1 min, and subsequently performed SDS-PAGE and electrotransferred onto polyvinylidene difluoride membranes. Then, the membranes were incubated with antibodies against Actin (1:200 diluted, Santa Cruz Biotechnology, C-2, sc-8432), Myc (1:200 diluted, Santa Cruz Biotechnology, 9E10, sc-40) or GFP (1:2000 diluted, Santa Cruz Biotech, sc-9996) for 8 h at 4 ˚C. The membranes were incubated for 20 min with horse radish peroxidase (HRP)-conjugated antibodies (1:6000 diluted, rabbit anti-mouse IgG, DAKO). HRP on the membrane was detected using the ECL Advance luminescence solution (GE Healthcare Life Science) according to the manufacturer’s instruction.

2.4. Measurement of aggregate positivity

To visualize EGFP-tagged proteins, a fluorescence microscope IX-51 (Olympus, Japan) with 20×/0.40 NA dry objective was used. At 16 h post-transfection, HeLa cells expressing EGFP-tagged αBC mutants were illuminated with the mercury light (U-LH100HGAPO). EGFP images were captured with a digital camera WRAYCAM-SR300 (WRAYMER, Japan) and WraySpect (WRAYMER, Japan). WRAYCAM-

SR300 was used through 0.35×c-mount lens. Based on the images, the percentage of the cells with aggregates in EGFP-positive cells was calculated. At least 800 cells were analyzed for each condition in every assay.

2.5. Statistical analysis

All data were expressed as means ± S.E.M. The data was accumulated under each condition from at least six independent experiments. For parametric all-pairs multiple comparisons in all figures, Tukey-test was used.

3. Results

3.1 The inability of the R106PfsX26 CLN6 mutant to prevent aggregation of the R120G αBC mutant

The R106PfsX26 (hereafter referred to as 106fsX) human CLN6 mutant is produced by a 1-bp insertion (c.316insC) causing a frame shift and a premature stop codon, identical to that identified in the *nclf* mouse, a naturally occurring model of CLN6 disease [14–17]. The detection of p62-positive aggregates in the brain of *nclf* mice prompted us to raise the possibility that CLN6's anti-aggregate activity is diminished by the 106fsX mutation, resulting in the accumulation of protein aggregates and in turn the development of CLN6 disease. To explore this possibility, we first determined if the 106fsX mutation indeed impairs CLN6's anti-aggregate activity toward the R120G αBC mutant. Aggregation of the R120G αBC mutant in HeLa cells was suppressed upon coexpression of Myc-tagged wild-type CLN6, as was demonstrated in our previous report (Fig. 1A,B). In contrast, the anti-aggregate activity was comparable between the 106fsX mutant- and the insertless vector-transfected cells. Immunoblot

analysis revealed that the band representing the Myc-tagged 106fsX mutant was dim relative to that of wild-type CLN6 (Fig. 1C), consistent with the previous finding that this mutant undergoes rapid degradation. Taken together, we concluded that the 106fsX mutant is unable to repress aggregation of the R120G αBC mutant due to a lack of anti-aggregate activity and/or relatively low expression levels, in support of our hypothesis that the malfunction of CLN6-driven protection system against protein aggregation causes CLN6 disease.

3.2. Requirement of the integrity of CLN6's third loop for its anti-aggregate activity

The inability of the 106fsX mutant to antagonize the R120G αBC mutant prompted us to probe the minimum N-terminal region of CLN6 required for its anti-aggregate activity. When coexpressed in HeLa cells, the N-terminal half of CLN6 (residues 1-162) suppressed aggregation of the R120G αBC mutant to a similar extent as wild-type CLN6 (Fig. 2 A,B). On the other hand, HeLa cells transfected with another CLN6 truncated mutant (residues 1-142) or the 106fsX mutant exhibited comparably high aggregate positivity, indicating that a region essential for CLN6's anti-aggregate activity lies somewhere between amino acid positions 142 and 162. In order to narrow down the responsible region, we replaced each of the amino-acid stretches 141-146, 147-151, 152-156 and 157-161, with five alanine residues for the subsequent coexpression assays. (Fig. 2C; 5A1-4). The protein level of the 5A2 mutant in transfected HeLa cells was extremely low as compared with that of the 5A1, 5A3, and 5A4 mutants (Fig. 2D). Furthermore, aggregate positivity of the 5A2 mutant-expressing cells was as high as that of the 106fsX mutant-expressing cells (Fig. 2E), showing that the structural integrity of the 147-151 amino-acid stretch is indispensable for the stability and anti-aggregate activity of CLN6. Considering that missense mutations at the positions 148 and 149 have been documented in patients with CLN6 disease, we then focused on the

middle three residues in the 147-151 stretch. The V148A/R149A/E150A triple mutation severely attenuated CLN6's anti-aggregate activity, as revealed by aggregate positivity of ~45% (Fig. 2C,F,G; 3A). In contrast, the S147A/N151A double mutation appeared not to significantly affect the activity (Fig. 2C,F,G; 2A), demonstrating the 148-150 amino-acid stretch is vital for CLN6 to prevent aggregation of the R120G αBC mutant.

3.3 The R149C substitution abolished CLN6's anti-aggregate activity toward the R120G αBC mutant

Situated in the middle of the 148-150 amino-acid stretch is R149, and its mutations to cysteine (R149C) and histidine (R149H) have been associated with CLN6 disease [18–20]. It thus might be that these two mutations attenuate CLN6's anti-aggregate activity to some extent, and that the resulting buildup of protein aggregates underlies the development of the disease. To explore this possibility, we examined if the two substitutions affect the ability of CLN6 to antagonize aggregation of the R120G αBC mutant. Comparably high aggregate positivity was displayed by the R149C mutant- and the 106fsX mutant-transfected cells (Fig 3A,B), indicating that the R-to-C substitution completely abrogates CLN6's anti-aggregate activity toward the R120G αBC mutant. On the other hand, the R149H mutant lowered the positivity to a similar degree as wild-type CLN6. We hence concluded that the R-to-C, but not the R-to-H, substitution at the position 149 nullifies the ability of CLN6 to repress the R120G αBC mutant from aggregating.

3.4 The R149C mutant retained residual anti-aggregate activity

The failure to block aggregation of the R120G αBC mutant led us to reason that the R149C mutant can exert little, if any, anti-aggregate activity toward physiological targets of CLN6, thereby underlying the CLN6 disease pathogenesis. It is, however, not feasible to explore this possibility because proteins that CLN6 acts on have been largely unknown. We then assessed if the R149C mutant could antagonize other pathogenic αBC mutants, such as D109H, G154S, and R157H, all of which have been reported in families diagnosed with αB-crystallinopathy [21–27]. Like the R120G αBC mutant, these αBC mutants fused to EGFP aggregated to varying extents, consistent with a previous report [12] (Fig. 4A-C). Unexpectedly, the R149C prevented aggregation of the G154S and R157H, but not of the D109H or R120G, αBC mutants (Fig. 4D). In contrast with the R149C mutant, the R149H mutant blocked all the four αBC mutants from aggregating. Together, we suggested that the R149C mutant is able to protect some, but not a full range, of CLN6's physiological targets from aggregating, and that proteins not protected by CLN6 mediate aggregate formation, triggering the pathogenic process in CLN6 disease.

4. Discussion

We previously demonstrated that CLN6 has the ability to prevent aggregation the R120G αBC mutant, a model aggregation-prone protein. Based on this finding, we hypothesized that a buildup of protein aggregates due to a loss of CLN6's anti-aggregate activity results in the development of CLN6 disease, a division of NCL. Little has been known about CLN6's target proteins with the exception of CRMP2, identified as a CLN6 binder through yeast two-hybrid screens [28]. Consequently, we cannot even examine if physiological targets of CLN6 indeed aggregate to become dysfunctional when deprived of CLN6-mediated protection and support. Faced with this limitation, we employed the four disease-causing αBC mutants in order to gain insight into

whether CLN6 is capable of countering a diverse array of aggregation-prone proteins. Patients with αB-crystallinopathy display various combinations of cataract, myopathy and cardiomyopathy, depending on which αBC mutant they inherit. The disparity in their clinical manifestations prompted us to reason that the four pathogenic αBC mutants differ from each other in their higher structures and accordingly help propagate distinct signals across the cytoplasm. In this regard, our data indicate that CLN6 can antagonize at least four separate proteins destined to spontaneously aggregate.

We showed that CLN6's third loop plays vital roles for its anti-aggregate activity. Amino acids 148-150 in the loop were particularly critical as their simultaneous replacement with three alanine residues induced a marked drop in the activity. These three residues are most likely to serve to meet conformational requirements for CLN6's functionality. Among the three amino acids, the position 149 is of great interest because two kinds of substitutions, R149C and R149H, have been described in patients with adult-onset CLN6 disease, collectively termed Kufs disease. The R149C mutant prevented aggregation of two out of the four pathogenic αBC mutants, prompting us to expect that not all of CLN6's physiological targets are protected from aggregating in individuals homozygous for the R149C substitution. Likewise, individuals homozygous for the 106fsX mutation, affected with late infantile-onset CLN6 disease, would also manifest a buildup of protein aggregates given that p62-positive protein aggregates were detected in the *nclf* mouse. It might thus be that the accumulation of protein aggregates entangling CLN6's targets is not just a shared feature of late infantile- and adult-onset CLN6 disease, but also a major cause of illness. Of note, impacts on the four αBC mutants showed that the R149C substitution attenuated CLN6's anti-aggregate activity less severely than the 106fsX mutation. Provided that antagonizing effects on the four pathogenic αBC mutants recapitulates what happens to physiological substrates of CLN6, a more diverse array of proteins could avoid aggregating in individuals homozygous for the R149C substitution relative to those for

the 106fsX mutation, producing the difference in clinical symptoms between the two CLN6 disease subtypes. Taken together, we propose that the extent to which CLN6's anti-aggregate activity is impaired would be a key determinant of the clinical course of CLN6 disease: virtually complete loss of the activity due to homozygosity of the 106fsX mutation leads to the development of late infantile-onset CLN6 disease, whereas the less severely impaired activity, resulting from homozygosity of the R149C substitution, contributes to adult-onset CLN6 disease.

The R149H substitution was documented, combined with the P297LfsX53 (hereafter referred to as 297fsX) mutation in patients with adult-onset CLN6 disease. We validated that the 297fsX CLN6 mutant also blocked the four pathogenic αBC mutants from aggregating (data not shown), suggesting that the CLN6-mediated preventive system against protein aggregation still operates in individuals with the R149H/297fsX compound heterozygosity, and that their clinical manifestations are attributable to impairment of an as-yet-unidentified function of CLN6 irrelevant to antagonizing protein aggregate formation. The success in countering the four αBC mutants, however, does not necessarily guarantee that a full range of CLN6's targets can avoid aggregating in patients with compound heterozygosity of the R149H/297fsX. The resulting protein aggregates and their accumulation in this setting could also be the primary cause of adult-onset CLN6 disease. If this was the case, CLN6-related Kufs disease would be etiologically categorized into at least two subdivisions: one is attributable to the impairment of CLN6's anti-aggregate activity, and the other is due to defects in as-yet-unidentified CLN6's functions, thereby accounting for why CLN6 disease is characterized by its heterogeneity in the age of onset and clinical course.

Our findings suggest that CLN6 disease is caused through either of the two distinct mechanisms: one involves the graded reduction in CLN6's anti-aggregate activity, and the other does not. We therefore propose that it is what amino acid residue replaces

key positions of CLN6, including R149, that governs which of the pathogenic mechanisms predominantly operates and which subdivision of CLN6 disease develops.

Acknowledgements

This work was supported by JSPS KAKENHI Grant Numbers JP18K07045 (T. Y.) and JP16J09784 (A. Y.).

References

[1] S.E. Mole, G. Michaux, S. Codlin, R.B. Wheeler, J.D. Sharp, D.F. Cutler, CLN6, which is associated with a lysosomal storage disease, is an endoplasmic reticulum protein, Exp. Cell Res. 298 (2004) 399–406. doi:10.1016/j.yexcr.2004.04.042.

[2] J. Alroy, T. Braulke, I.A. Cismondi, J.D. Cooper, D. Creegan, M. Elleder, C. Kitzmüller, R. Kohan, A. Kohlschütter, S.. Mole, I. Noher de Halac, R. Pfannl, A. Quitsch, A. Schulz, CLN6, in: Neuronal Ceroid Lipofuscinoses (Batten Dis., Oxford University Press, 2011: pp. 159–175. doi:10.1093/med/9780199590018.003.0010.

[3] K. Kollmann, K. Uusi-Rauva, E. Scifo, J. Tyynelä, A. Jalanko, T. Braulke, Cell biology and function of neuronal ceroid lipofuscinosis-related proteins, Biochim. Biophys. Acta - Mol. Basis Dis. 1832 (2013) 1866–1881. doi:10.1016/j.bbadis.2013.01.019.

[4] V. Warrier, M. Vieira, S.E. Mole, Genetic basis and phenotypic correlations of the neuronal ceroid lipofusinoses, Biochim. Biophys. Acta - Mol. Basis Dis. 1832 (2013) 1827–1830. doi:10.1016/j.bbadis.2013.03.017.

[5] D.N. Palmer, L.A. Barry, J. Tyynelä, J.D. Cooper, NCL disease mechanisms, Biochim. Biophys. Acta - Mol. Basis Dis. 1832 (2013) 1882–1893.

doi:10.1016/j.bbadis.2013.05.014.

[6] J. Cárcel-Trullols, A.D. Kovács, D.A. Pearce, Cell biology of the NCL proteins: What they do and don't do, Biochim. Biophys. Acta - Mol. Basis Dis. 1852 (2015) 2242–2255. doi:10.1016/j.bbadis.2015.04.027.

[7] H.R. Nelvagal, J. Lange, K. Takahashi, M.A. Tarczyluk-Wells, J.D. Cooper, Pathomechanisms in the neuronal ceroid lipofuscinoses, Biochim. Biophys. Acta - Mol. Basis Dis. (2019) 165570. doi:10.1016/j.bbadis.2019.165570.

[8] E.S. Butz, U. Chandrachud, S.E. Mole, S.L. Cotman, Moving towards a new era of genomics in the neuronal ceroid lipofuscinoses, Biochim. Biophys. Acta - Mol. Basis Dis. (2019) 165571. doi:10.1016/j.bbadis.2019.165571.

[9] S.F. Berkovic, K.L. Oliver, L. Canafoglia, P. Krieger, J.A. Damiano, M.S. Hildebrand, M. Morbin, D.F. Vears, V. Sofia, L. Giuliano, B. Garavaglia, A. Simonati, F.M. Santorelli, A. Gambardella, A. Labate, V. Belcastro, B. Castellotti, C. Ozkara, A. Zeman, J. Rankin, S.E. Mole, U. Aguglia, M. Farrell, S. Rajagopalan, A. McDougall, S. Brammah, F. Andermann, E. Andermann, H.H.M. Dahl, S. Franceschetti, S. Carpenter, Kufs disease due to mutation of CLN6: Clinical, pathological and molecular genetic features, Brain. 142 (2019) 59–69. doi:10.1093/brain/awy297.

[10] J. Tyynelä, A.E. Lehesjoki, Kufs or not Kufs: Challenging diagnostics of a rare adult-onset neurodegenerative disease, Brain. 142 (2019) 2–5. doi:10.1093/brain/awy312.

[11] A. Yamashita, Y. Hiraki, T. Yamazaki, Identification of CLN6 as a molecular entity of endoplasmic reticulum-driven anti-aggregate activity, Biochem. Biophys. Res. Commun. 487 (2017) 917–922. doi:10.1016/j.bbrc.2017.05.002.

[12] D. Selcen, A.G. Engel, Myofibrillar Myopathy Caused by Novel Dominant Negative αB-Crystallin Mutations, Ann. Neurol. 54 (2003) 804–810. doi:10.1002/ana.10767.

[13] S. Yamamoto, A. Yamashita, N. Arakaki, H. Nemoto, T. Yamazaki, Prevention of aberrant protein aggregation by anchoring the molecular chaperone αB-crystallin to the endoplasmic reticulum, Biochem. Biophys. Res. Commun. 455 (2014) 241–245. doi:10.1016/J.BBRC.2014.10.151.

[14] R.T. Bronson, L.R. Donahue, K.R. Johnson, A. Tanner, P.W. Lane, J.R. Faust, Neuronal ceroid lipofuscinosis (nclf), a new disorder of the mouse linked to chromosome 9, Am. J. Med. Genet. 77 (1998) 289–297. doi:10.1002/(SICI)1096-8628(19980526)77:4<289::AID-AJMG8>3.0.CO;2-I.

[15] R.B. Wheeler, J.D. Sharp, R.A. Schultz, J.M. Joslin, R.E. Williams, S.E. Mole, The gene mutated in variant late-infantile neuronal ceroid lipofuscinosis (CLN6) and in nclf mutant mice encodes a novel predicted transmembrane protein, Am. J. Hum. Genet. 70 (2002) 537–542. doi:10.1086/338708.

[16] H. Gao, R.M.N. Boustany, J.A. Espinola, S.L. Cotman, L. Srinidhi, K.A. Antonellis, T. Gillis, X. Qin, S. Liu, L.R. Donahue, R.T. Bronson, J.R. Faust, D. Stout, J.L. Haines, T.J. Lerner, M.E. MacDonald, Mutations in a novel CLN6-encoded transmembrane protein cause variant neuronal ceroid lipofuscinosis in man and mouse, Am. J. Hum. Genet. 70 (2002) 324–335. doi:10.1086/338190.

[17] A.K. Kurze, G. Galliciotti, C. Heine, S.E. Mole, A. Quitsch, T. Braulke, Pathogenic mutations cause rapid degradation of lysosomal storage disease-related membrane protein CLN6, Hum. Mutat. 31 (2010) E1163-74. doi:10.1002/humu.21184.

[18] M. Kousi, A.E. Lehesjoki, S.E. Mole, Update of the mutation spectrum and clinical correlations of over 360 mutations in eight genes that underlie the neuronal ceroid lipofuscinoses, Hum. Mutat. 33 (2012) 42–63. doi:10.1002/humu.21624.

[19] A. Jilani, D. Matviychuk, S. Blaser, S. Dyack, J. Mathieu, A.N. Prasad, C. Prasad, L. Kyriakopoulou, S. Mercimek-Andrews, High diagnostic yield of direct

Sanger sequencing in the diagnosis of neuronal ceroid lipofuscinoses, JIMD Rep. 50 (2019) 20–30. doi:10.1002/jmd2.12057.

[20] T. Arsov, K.R. Smith, J. Damiano, S. Franceschetti, L. Canafoglia, C.J. Bromhead, E. Andermann, D.F. Vears, P. Cossette, S. Rajagopalan, A. McDougall, V. Sofia, M. Farrell, U. Aguglia, A. Zini, S. Meletti, M. Morbin, S. Mullen, F. Andermann, S.E. Mole, M. Bahlo, S.F. Berkovic, Kufs disease, the major adult form of neuronal ceroid lipofuscinosis, caused by mutations in cln6, Am. J. Hum. Genet. 88 (2011) 566–573. doi:10.1016/j.ajhg.2011.04.004.

[21] P. Vicart, A. Caron, P. Guicheney, Z. Li, M.C. Prévost, A. Faure, D. Chateau, F. Chapon, F. Tomé, J.M. Dupret, D. Paulin, M. Fardeau, A missense mutation in the αb-crystallin chaperone gene causes a desmin-related myopathy, Nat. Genet. 20 (1998) 92–95. doi:10.1038/1765.

[22] N. Inagaki, T. Hayashi, T. Arimura, Y. Koga, M. Takahashi, H. Shibata, K. Teraoka, T. Chikamori, A. Yamashina, A. Kimura, αB-crystallin mutation in dilated cardiomyopathy, Biochem. Biophys. Res. Commun. 342 (2006) 379–386. doi:10.1016/j.bbrc.2006.01.154.

[23] A. Pilotto, N. Marziliano, M. Pasotti, M. Grasso, A.M. Costante, E. Arbustini, αB-Crystallin mutation in dilated cardiomyopathies: Low prevalence in a consecutive series of 200 unrelated probands, Biochem. Biophys. Res. Commun. 346 (2006) 1115–1117. doi:10.1016/j.bbrc.2006.05.203.

[24] P. Reilich, B. Schoser, N. Schramm, S. Krause, J. Schessl, W. Kress, J. Müller-Höcker, M.C. Walter, H. Lochmuller, The p.G154S mutation of the alpha-B crystallin gene (CRYAB) causes late-onset distal myopathy, Neuromuscul. Disord. 20 (2010) 255–259. doi:10.1016/j.nmd.2010.01.012.

[25] A. Sanbe, Molecular mechanisms of α-crystallinopathy and its therapeutic strategy, Biol. Pharm. Bull. 34 (2011) 1653–1658. doi:10.1248/bpb.34.1653.

[26] S. Sacconi, L. Féasson, J.C. Antoine, C. Pécheux, R. Bernard, A.M. Cobo, A.

Casarin, L. Salviati, C. Desnuelle, A. Urtizberea, A novel CRYAB mutation resulting in multisystemic disease, Neuromuscul. Disord. 22 (2012) 66–72. doi:10.1016/j.nmd.2011.07.004.

[27] E.S. Gerasimovich, S. V. Strelkov, N.B. Gusev, Some properties of three αB-crystallin mutants carrying point substitutions in the C-terminal domain and associated with congenital diseases, Biochimie. 142 (2017) 168–178. doi:10.1016/j.biochi.2017.09.008.

[28] J.W. Benedict, A.L. Getty, T.M. Wishart, T.H. Gillingwater, D.A. Pearce, Protein product of CLN6 gene responsible for variant late-onset infantile neuronal ceroid lipofuscinosis interacts with CRMP-2, J. Neurosci. Res. 87 (2009) 2157–2166. doi:10.1002/jnr.22032.

Figure legends

Figure 1. The R106PfsX26 CLN6 mutant was unable to prevent aggregate formation of the R120G αBC mutant.

(A) HeLa cells were cotransfected with the EGFP-tagged R120G αBC mutant (R120G) in combination with either empty vector (Ev), wild type CLN6 (CLN6) or R106PfsX26 CLN6 mutant (106fsX). Images were captured at 16 hr post-transfection. Scale bars: 20 μm. (B) Based on (A), the percentages of the cells with aggregates were calculated. The data represent mean ± SEM of ten separate experiments. $*p < 0.05$. (C) The whole cell lysates from (A) were immunoblotted with antibodies against Myc and Actin.

Figure 2. The 148-150 amino-acid stretch was vital for CLN6's anti-aggregate activity.

(A) Anti-aggregate activity of two truncated CLN6 mutants (1-142 and 1-162) were determined. The HeLa cells were cotransfected with the R120G αBC mutant (R120G)

in combination with either wild-type CLN6, 1-162, 1-142 or 106fsX. The data represent mean ± SEM of six independent experiments. *$p < 0.05$. (B) The whole cell lysates from (A) were immunoblotted with antibodies against Myc and Actin. (C) Schematic representation of wild-type CLN6 and its mutants. (D) The whole cell lysates from HeLa cells cotransfected with R120G αBC mutant in combination with either wild-type CLN6, 5A1, 5A2, 5A3, 5A4 or 106fsX were immunoblotted with antibodies against Myc and Actin. (E) The HeLa cells were cotransfected as in (D), and then imaged. The percentages of the cells with aggregates were calculated as in Fig. 1(B). The data represent mean ± SEM of eight independent experiments. *$p < 0.05$. (F) The HeLa cells were cotransfected with the R120G αBC mutant (R120G) in combination with either wild-type CLN6, 3A, 2A or 5A2. The data represent mean ± SEM of seven independent experiments. *$p < 0.05$. (G) The whole cell lysates from (F) were immunoblotted with antibodies against Myc and Actin.

Figure 3. The R149C substitution abolished CLN6's anti-aggregate activity toward the R120G αBC mutant.

(A) The HeLa cells were co-transfected with the R120G αBC mutant (R120G) in combination with either wild-type CLN6, R149C, R149H or 106fsX. The percentages of the cells with aggregates were calculated as in Fig. 1(B). The data represent mean ± SEM of ten independent experiments. *$p < 0.05$. (B) Whole cell lysates from (A) were immunoblotted with antibodies against Myc and Actin.

Figure 4. The R149C mutant retained residual anti-aggregate activity.

(A) The cells were individually transfected with the indicated αBC mutants (D109H, R120G, G154S, R157H). At 16h post transfection, the cells were imaged with a fluorescence microscope. Scale bars: 20 μm. (B) Based on (A), the percentages of the cells with aggregates were calculated as in Fig. 1(B). The data represent mean ±

SEM of six independent experiments. *$p < 0.05$. (C) The whole cell lysates from the cells transfected with either empty vector (Ev) or EGFP-tagged αBC mutants were immunoblotted with antibodies against GFP and Actin. (D) The cells were cotransfected with the indicated combination of the EGFP-tagged αBC mutants and Myc-tagged wild-type CLN6 and its mutants. The percentages of the cells with aggregates were calculated as in Fig. 1(B). The data represent mean ± SEM of six independent experiments. *$p < 0.05$.

Fig.1

A

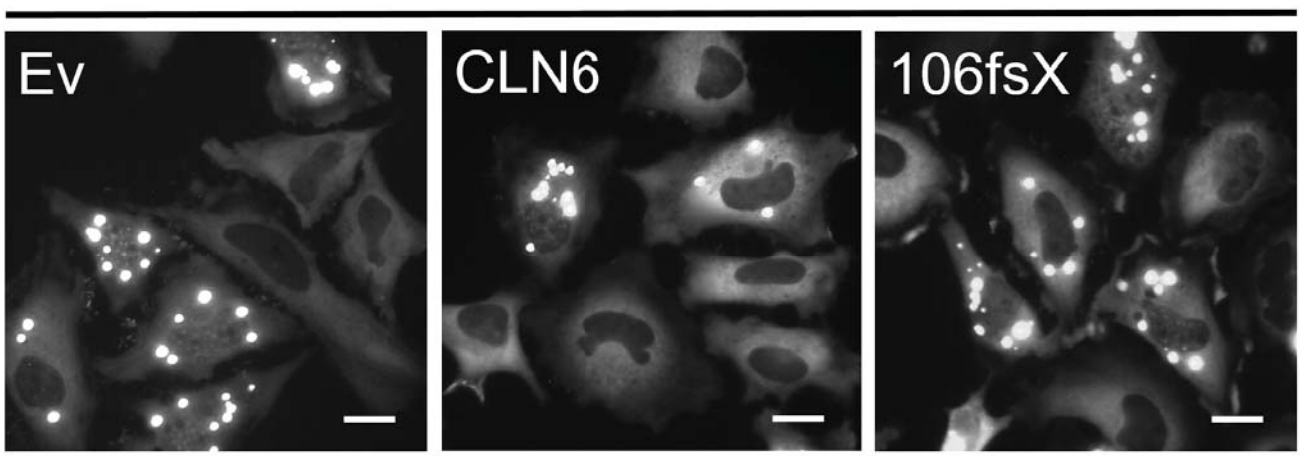
+R120G
Ev
CLN6
106fsX

B

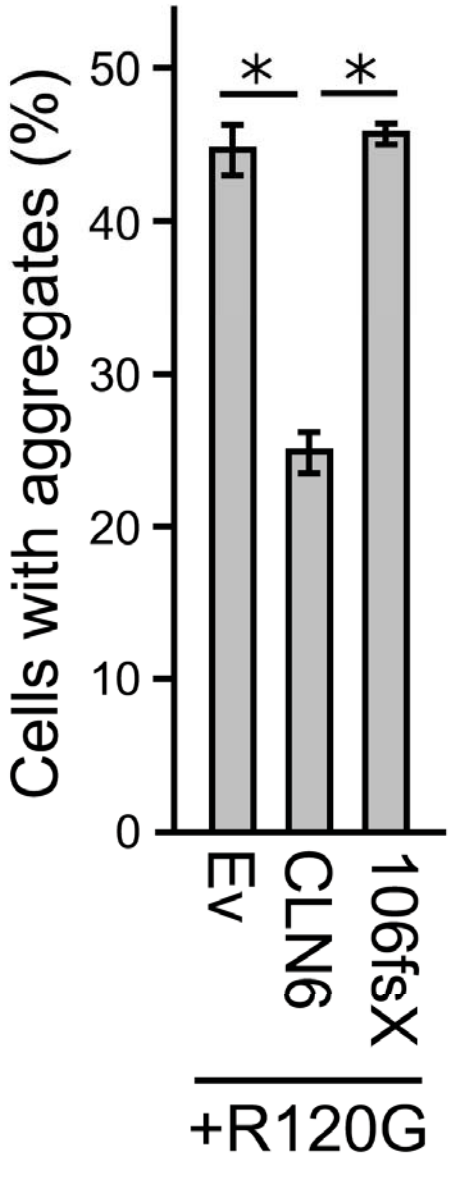
Cells with aggregates (%)
50
40
30
20
10
0
*
*
Ev
CLN6
106fsX
+R120G

C

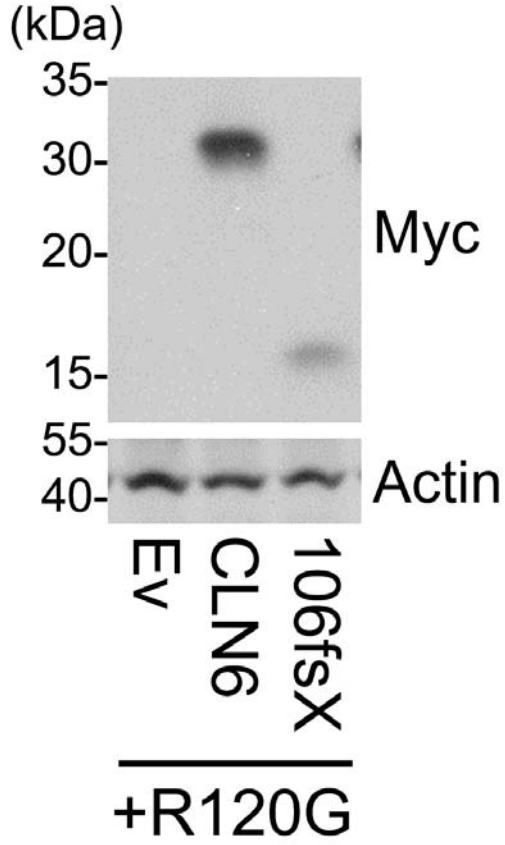
(kDa)
35-
30-
20-
15-
55-
40-
Myc
Actin
Ev
CLN6
106fsX
+R120G

Fig.2

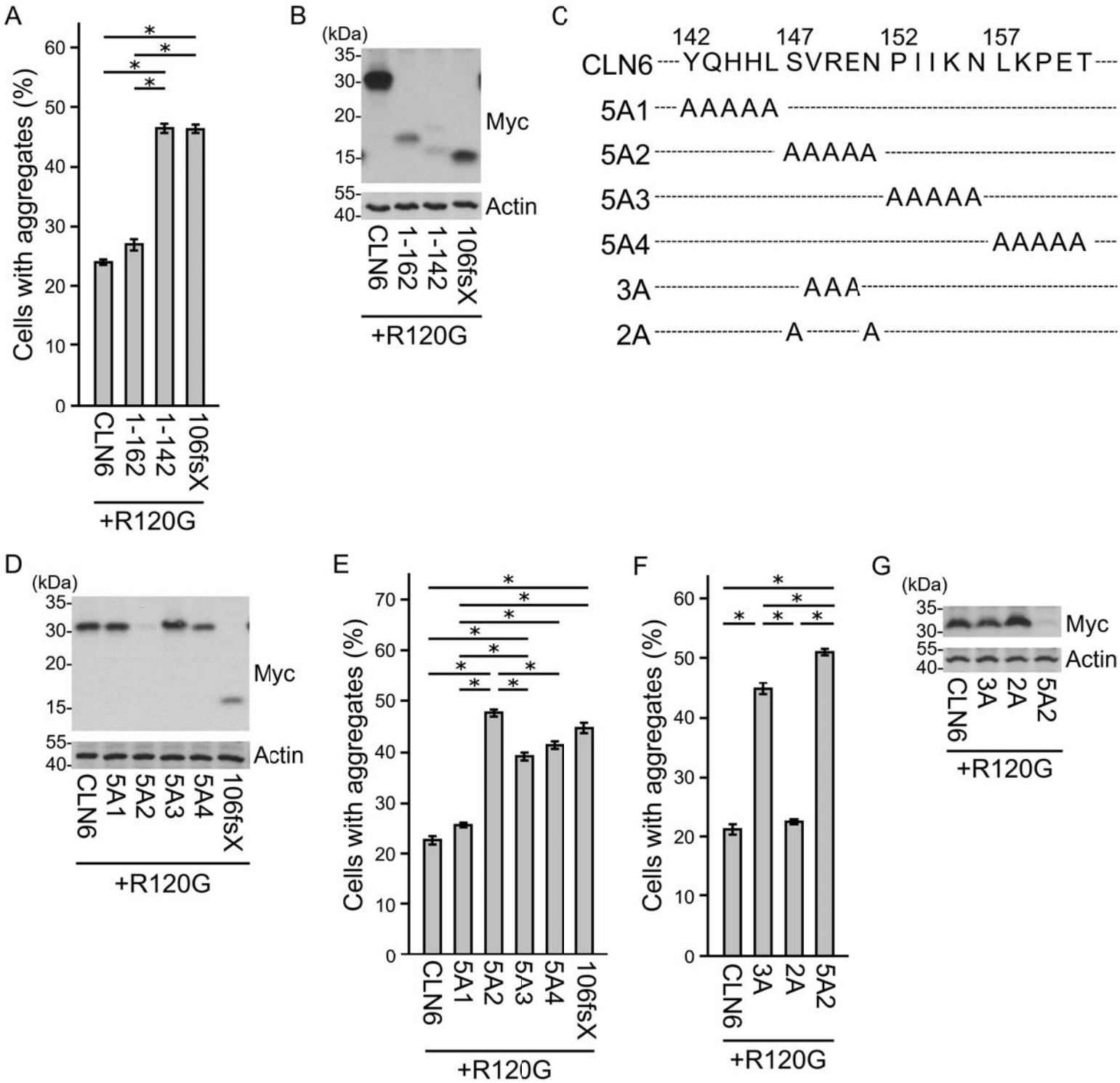
A
Cells with aggregates (%)
CLN6
1-162
1-142
106fsX
+R120G
B
(kDa)
Myc
Actin
CLN6
1-162
1-142
106fsX
+R120G
C
142 147 152 157
CLN6 YQHHL SVREN PIIKN LKPET
5A1 AAAAA
5A2 AAAAA
5A3 AAAAA
5A4 AAAAA
3A AAA
2A A A
D
(kDa)
Myc
Actin
CLN6
5A1
5A2
5A3
5A4
106fsX
+R120G
E
Cells with aggregates (%)
CLN6
5A1
5A2
5A3
5A4
106fsX
+R120G
F
Cells with aggregates (%)
CLN6
3A
2A
5A2
+R120G
G
(kDa)
Myc
Actin
CLN6
3A
2A
5A2
+R120G

Fig.3

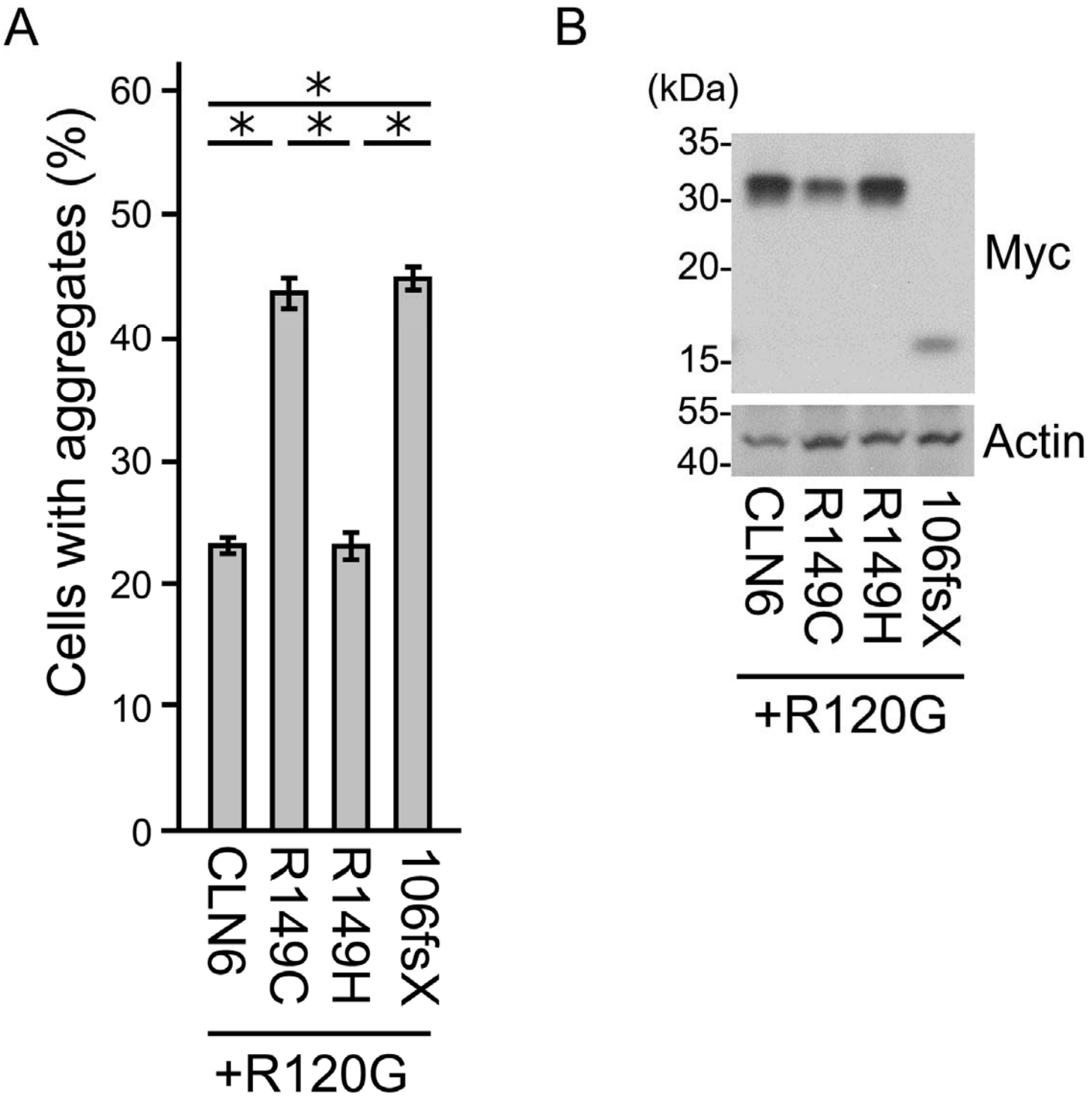
A
Cells with aggregates (%)
60
50
40
30
20
10
0
*
*
*
*
CLN6
R149C
R149H
106fsX
+R120G
B
(kDa)
35-
30-
20-
15-
55-
40-
Myc
Actin
CLN6
R149C
R149H
106fsX
+R120G

Fig.4

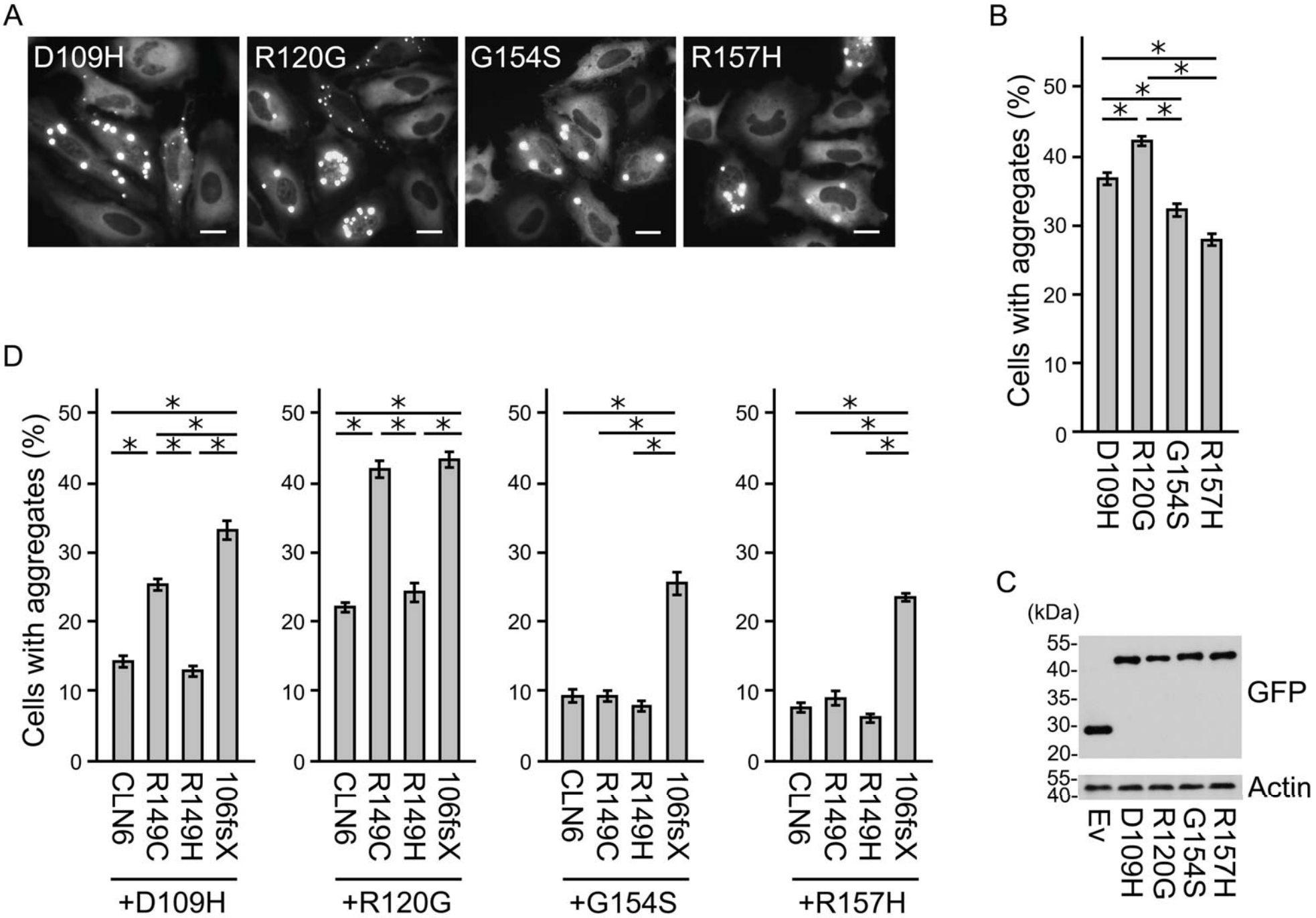
A
D109H
R120G
G154S
R157H
B
Cells with aggregates (%)
0
10
20
30
40
50
D109H
R120G
G154S
R157H
C
(kDa)
55-
40-
35-
30-
20-
55-
40-
GFP
Actin
Ev
D109H
R120G
G154S
R157H
D
Cells with aggregates (%)
CLN6
R149C
R149H
106fsX
+D109H
+R120G
+G154S
+R157H

Supplementary tables

Table S1 The following primer sets are used in generating expression constructs.

Target		Sequence
D109H	Fragment 1	5’-CGGAATTCACCATGGACATCGCCATCC-3’
		5’-GATGAAACCATGTTCGTGCTGGCGCTCTTC-3’
	Fragment 2	5’-CAGGAACATGGTTTCATCTCCAGGGAGTTC-3’
		5’-CGGTCGACCATTTCTTGGGGGCTGCG-3’
G154S	Fragment 1	5’-CGGAATTCACCATGGACATCGCCATCC-3’
		5’-GGTGCGCTCAGGGCTAGAGACCTGTTTCCT-3’
	Fragment 2	5’-AGCCCTGAGCGCACCATTCCCATCACCCGT-3’
		5’-CGGTCGACCATTTCTTGGGGGCTGCG-3’
R157H	Fragment 1	5’-CGGAATTCACCATGGACATCGCCATCC-3’
		5’-GATGGGAATGGTGTGCTCAGGGCCAGAGAC-3’
	Fragment 2	5’-ACACCATTCCCATCACCCGTGAAGAGAAGC-3’
		5’-CGGTCGACCATTTCTTGGGGGCTGCG-3’

Table S2 The following primers are used in generating the R106PfsX26 CLN6 mutant.

Primer	Sequence
316insC-Fwd	5’-GTCCCCCCCGCACCCTGCCACGCTC-3’
316insC-Rev	5’-GGGTGCGGGGGGGACCGCTCGATGA-3’
106fsX-Fwd	5’-TGGTGGGGAATTCTGCAGATATCCA-3’
106fsX-Rev	5’-CAGAATTCCCCACCAGGTGGATGCTG-3’

Table S3 The following primers sets are used in generating the CLN6 mutants.

Target	Sequence
1-142	5’-GGCTACTGGAATTCTGCAGATATCCAGCACAGT-3’
	5’-AGAATTCCAGTAGCCACTGAAGAGCAGGCGGTG-3’
1-162	5’-ACGCTGTGGAATTCTGCAGATATCCAGCACAGT-3’
	5’-AGAATTCCACAGCGTCTCCGGCTTGAGATTCTT-3’
5A1	5’-GCTGCAGCTGCTGCTTCTGTCCGTGAGAACCCC-3’
	5’-AGCAGCAGCTGCAGCGCCACTGAAGAGCAGGCG-3’
5A2	5’-GCTGCAGCTGCTGCTCCCATCATCAAGAATCTC-3’
	5’-AGCAGCAGCTGCAGCCAGGTGGTGCTGGTAGCC-3’
5A3	5’-GCTGCAGCTGCTGCTCTCAAGCCGGAGACGCTG-3’
	5’-AGCAGCAGCTGCAGCGTTCTCACGGACAGACAG-3’
5A4	5’-GCAGCAGCAGCAGCACTGATCGACTCCTTTGAG-3’
	5’-TGCTGCTGCTGCTGCATTCTTGATGATGGGGTT-3’
3A	5’-TCTGCTGCTGCTAACCCCATCATCAAG-3’
	5’-GTTAGCAGCAGCAGACAGGTGGTGCTG-3’
2A	5’-CTGTCGCTGCGAACCCCATCATCAAGAA-3’
	5’-GGTTCGCAGCGACAGACAGGTGGTGCTG-3’
R149C	5’-TCTGTCTGTGAGAACCCCATCATCAAG-3’
	5’-GTTCTCACAGACAGACAGGTGGTGCTG-3’
R149H	5’-TCTGTCCATGAGAACCCCATCATCAAG-3’
	5’-GTTCTCATGGACAGACAGGTGGTGCTG-3’